ELSEVIER

Materials Science and Engineering A 488 (2008) 562–568

MATERIALS SCIENCE & ENGINEERING A

www.elsevier.com/locate/msea

Fracture toughness evaluation using Palmqvist crack models on AISI 1045 borided steels

I. Campos [a,*], R. Rosas [b], U. Figueroa [c], C. VillaVelázquez [a], A. Meneses [a], A. Guevara [d]

[a] *Instituto Politécnico Nacional, SEPI-ESIME U.P., Adolfo López Mateos, Zacatenco, México D.F. 07738, Mexico*
[b] *Instituto de Investigaciones en Materiales, UNAM, Circuito Exterior S/N Ciudad Universitaria, México D.F. 04510 Mexico*
[c] *Tecnológico de Monterrey Campus Estados de México, Carretera al Lago de Guadalupe, km. 3.5, Atizapán Edo, de México 52926, Mexico*
[d] *Imperial College London, South Kensington Campus, London SW7 2AZ, United Kingdom*

Received 16 October 2007; received in revised form 17 November 2007; accepted 30 November 2007

Abstract

The present study evaluates the fracture toughness on Fe_2B borided layers. Formation of the layers was obtained by means of the paste boriding process on an AISI 1045 steel surface. The treatment was carried out at temperatures of 1123, 1173, 1223 and 1273 K for 8 h using a 4 mm thickness layer of boron carbide paste over the material surface. A Vickers microhardness tester was used to generate microcracks under loads of 1.9, 2.9, 4.9 and 9.8 N at different indentation distances across the thickness of the iron boride layer. The applied loads and the crack lengths generated from the corners of the indentations were set as the experimental parameters, using two Palmqvist cracks models, for the evaluation of the fracture toughness. Finally, the fracture toughness results in the borided layers were analyzed based on the different distances from the surface, microindentation loads and the treatment temperatures of the paste boriding process.

Keywords: Paste boriding; Boride layers; Fracture toughness; Palmqvist cracks; Microindentation tests

1. Introduction

The paste boriding process is the surface boron saturation of metals and alloys with the purpose of increasing the hardness, wear and corrosion resistance of engineering components. Due to this process, interstitial compounds are formed, known as rhombic FeB and tetragonal boride Fe_2B, which form columnar crystals that grow in a preferential direction [0 0 1] due to the maximum density of boron atoms in that direction. The formed coatings depend on the boron potential at the external surface of the substrate. It is known that media with a low or intermediate boron potential (as compared to more powerful ones) allow single Fe_2B layers to form [1,2]. The formation of FeB phase requires a high potential of boron to an extent also depending on the concentration of alloying elements in the steel, especially a high content of chromium, nickel and carbon [3].

Paste boriding is an alternative method of sample treatment when the manual work required in powder boriding needs to be decreased. In addition, its advantage lies in high volumes of work and in selective treatments. Boron carbide paste consists of B_4C (approximately 76 wt% boron) and cryolithe (Na_3AlF_6, flux additive). A maximum of 10–15% of water can be added without impairing the boriding effect. The control of boron potential is possible according to the thickness of the boron carbide paste that covers the work piece and to the preparation of water–powder mixture. An inert atmosphere is needed inside the furnace, fixing a nitrogen and hydrogen combination of 90:10 or 95:5 or pure argon. The controlled atmosphere used in the paste boriding process determines the thicknesses of the borided layers, having more depth in comparison with the powder boriding process. On the other hand, the paste boriding process is favored by its low cost, quality of products, and flexibility during the process [1–5]. Typically, boronized parts have been used with good results in various industrial areas. These results increase the life-

* Corresponding author. Tel.: +52 55 57296000x54768; fax: +52 55 57296000x54589.
E-mail address: icampos@ipn.mx (I. Campos).

0921-5093/$ – see front matter © 2008 Elsevier B.V. All rights reserved.
doi:10.1016/j.msea.2007.11.082

time of machine elements and the serviceable lives of working tools.

One important mechanical parameter in design is the fracture toughness value. The method of microindentation-induced fracture in brittle materials is a nondestructive and simple technique, which requires solely a flat and polished surface. The cracks produced by mechanical contact between the indenter and the material surface essentially depend on the geometry of the indenter and the applied load.

The cracks geometry models, radial-median and Palmqvist types, have been used in the determination of the fracture toughness in ceramic materials. The theoretical foundation of these models is based on classic concepts of Linear Elastic Fracture Mechanics (LEFM) (see [6,7,24] and references therein). Many derivations make assumptions about the plastically deformed damage zone underneath the indentation. The damage zone is modeled by an expanding cavity in the solid. The stress distribution from the expanding cavity is in turn converted to an equivalent force that acts to open the median or Palmqvist cracks. Other models have the plastic zone acting as a wedge or a spring.

For the Palmqvist cracks regime (Fig. 1(a)), it has been determined, for small loads, that the relation between the half diagonal length of the indentation (l) and the crack length generated at the corners of the indentation (g) must be ≤ 3. It would seem reasonable to assume that, for thin brittle layers on relatively tough substrates (borided steels), it would be more appropriate to use the relationships based on the Palmqvist crack morphology, as this model is based on cracking initiating at the surface where the material is more brittle.

Also, the relations used by other researchers [8–11], to define the fracture toughness of borided layers are based on equations valid for radial-mean cracks, nevertheless, the reason for this consideration has not thoroughly been explained.

The present study evaluates the fracture toughness (K_c) of Fe_2B boride layers formed at the surface of AISI 1045 steels using two Palmqvist crack models proposed by Laugier and Niihara et al. [13,14]. The K_c values obtained by both models are compared with the applied load tests, the different distances from the surface of the borided samples and the treatment temperatures of the paste boriding process.

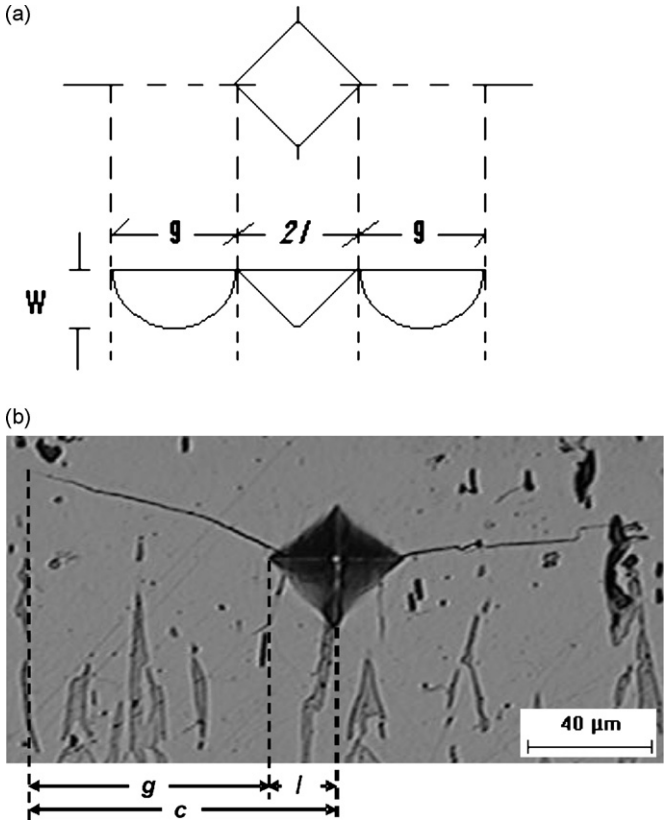

Fig. 1. (a) Palmqvist cracks produced by Vickers indentation and (b) Palmqvist microcracks produced at the corners of the indentation on the boride Fe_2B layer.

2. Experimental procedure

2.1. Paste boriding process

Cylindrical samples of AISI 1045 whose chemical composition is 0.43–0.50% C, 0.6–0.9% Mn, 0.040% P, 0.050% S, were cut, machined and recrystallized for 1 h at 923 K. Afterwards, the samples were placed in acrylic molds for the impregnation of the boron carbide paste (water/paste relation of 0.2) with a layer thickness of 4 mm, over the sample surfaces. It was necessary to dry the samples inside a conventional furnace at 373 K to eliminate any water residues so that the diffusion process could be done in an effective way. The paste boriding process was carried out at the temperatures of 1123, 1173, 1223 and 1273 K under a pure argon atmosphere in a conventional furnace with a constant time of 8 h for each temperature. Once the treatment was finished, the samples were oil-quenched, cross-sectioned for metallographic preparation and finally, characterized using an optic microscope with the aid of the MSQ image analyzer. A minimum of 25 measurements of the boride layer thicknesses was done at different zones of the samples.

2.2. Vickers microindentation fracture toughness tests

Vickers microindentation fracture toughness tests were carried out with a HVS 1000 microhardness tester employing ASTM E384 standard. The indentation load varied from 1.9 to 9.8 N applied at 15, 25, 35, 45, 55 and 65 μm from the borided steel surface. 10 measurements were taken for each distance, load and treatment temperature of the boriding process. Notice that the distances from the surface are selected in accordance with the Fe_2B layer thicknesses. In some cases, depending on the growth and the saw-toothed morphology of the boride layer, the indentation area is close to the spikes of the Fe_2B/substrate interphase. Also, when the temperature increases, the indentation area is closed towards the surface of the boride layer.

For the fracture toughness values, both Vickers diagonals (l) and crack lengths (g) were measured in a Olympus GX 51 microscope using a 50× and 100× magnifications (Fig. 1(b)). *Measurement thickness* tool of the MSQ Plus Software was employed to carried out the measurements. The Young modulus used for the borided layers was 290 GPa [12]. Finally, the Palmqvist crack models proposed by Laugier [13] (PI) and

Table 1
Palmqvist crack models used for the evaluation of the fracture toughness

Equation	References
$K_c = k^p \left(\frac{g}{l}\right)^{-1/2} \left(\frac{E}{H}\right)^{2/3} \frac{P}{c^{3/2}}$	[13]
$\left(\frac{K_c\phi}{H^{1/2}}\right) \left(\frac{H}{E\phi}\right)^{2/5} = 0.048 \left(\frac{g}{l}\right)^{-1/2}$	[14]

K_c, fracture toughness; E, Young modulus; H, microhardness; P, applied load; g, microcrack length; l, half diagonal length of the microindentation; ϕ, constraint factor ≈ 3; k^p, 0.015; c, total crack length.

Niihara et al. [14] (PII), illustrated in Table 1, were used to determine the fracture toughness of Fe_2B boride layers.

3. Results and discussions

The paste boriding process was designed to obtain a compact and continuous Fe_2B boride layer at the surface of AISI 1045 steels. The Fe_2B/substrate interphase shows a saw-toothed morphology (Fig. 2), while the layer thicknesses are 46 ± 4 μm at 1123 K and 141 ± 6 μm at 1273 K.

The mechanism of boron diffusion through the boride crystals occurs more readily when the atoms jump between neighboring lattice positions along the boron atoms which are connected in chains [15–17]. In order to allow the above-mentioned diffusion mechanism, a part of the lattice positions in the boron atom chains must be vacant. As a result of this diffusion mechanism the boride crystals, which are arranged with their boron atom chains parallel to the non-metal diffusion direction, grow more quickly than the others. The preferred orientation of crystals constituting the surface layer obtained by boriding steels also depends on the experimental parameters of the process. Borides produced by the boriding process presented a strong ⟨0 0 1⟩ growth texture. The growth of the boride grains with other orientations was slower and soon suppressed because their growth met other grains, resulting in a ⟨0 0 1⟩ texture structure.

The sharp indenters (conic or pyramidal) are normally used for the analysis of fracture toughness in opaque ceramic materials because the contact pressure is independent of the indentation size and the failure propagates from the corners of the residual impression. The number of indentations at the boride layers was established by three experimental parameters: the boride layer thickness, the indentation impression size, and the applied load. Besides, in order to obtain representative microhardness values of the Fe_2B iron boride, the indentations must not be close to the layer/substrate interphase. The set of microindentations tests at 1223 K with four different applied loads, 1.96, 2.9, 4.9 and 9.8 N are presented in Fig. 3.

Likewise, it is recommendable to use the true hardness number (load-independent) to determine the fracture toughness of the boride phase [18] and to eliminate the effect of the apparent hardness into the indentation fracture toughness equations.

According to the results obtained and shown in Fig. 4, the true hardness number of the Fe_2B layer decreases with increasing the test load at different distances from the borided steel surface. It is evident that the Vickers microhardness measurements, with applied loads of 4.9 and 9.8 N, are influenced by the indentation crack formation. In fact, since the cracks mainly occur during the loading, a portion of the energy that is used to create the indentation size will be dissipated by the crack formation [19]. In this case, the crack formation has influence in the indentation size of the Vickers impression at the applied loads of 4.9 and 9.8 N. Also, the true hardness values are influenced by the different distances from the surface of the borided samples. This behavior is explained with the residual stresses induced by thermal gradients. Babushkin and Polyakov [20] show that the

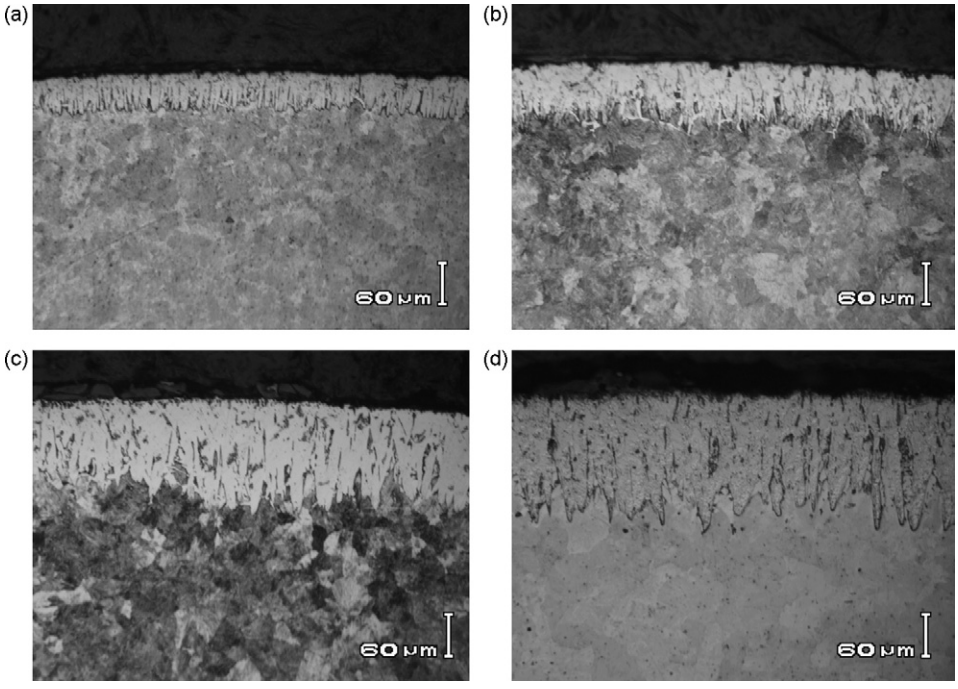

Fig. 2. Cross-sectional views of AISI 1045 borided steels with 8 h of treatment time at the temperatures of: (a) 1123 K, (b) 1173 K, (c) 1223 K and (d) 1273 K.

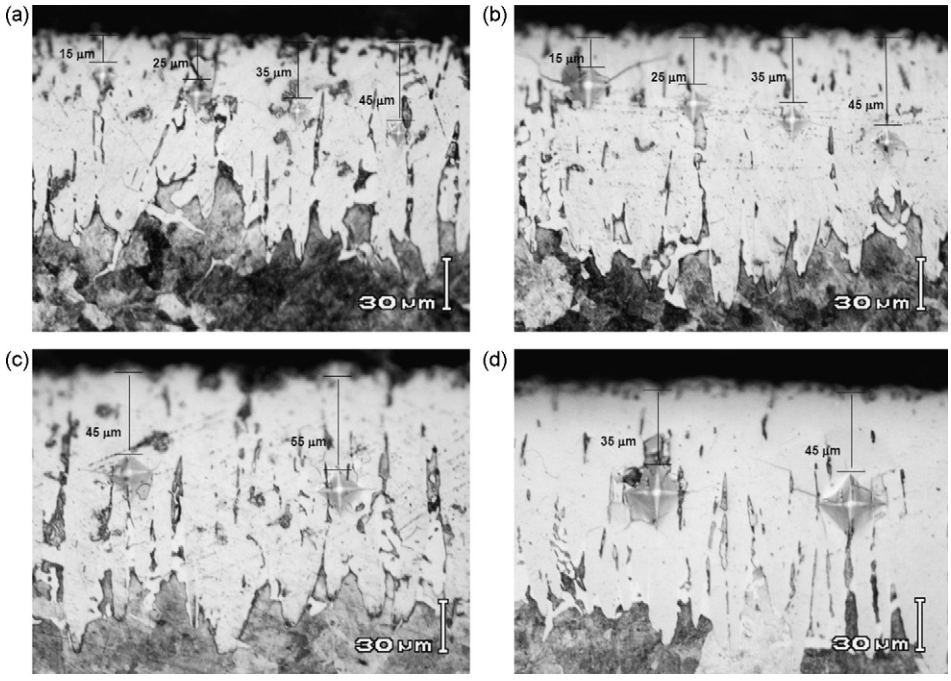

Fig. 3. Vickers microindentations fracture toughness tests on borided AISI 1045 steel samples at 1223 K with loads of: (a) 1.9 N, (b) 2.9 N, (c) 4.9 N and (d) 9.8 N. Magnification 500×.

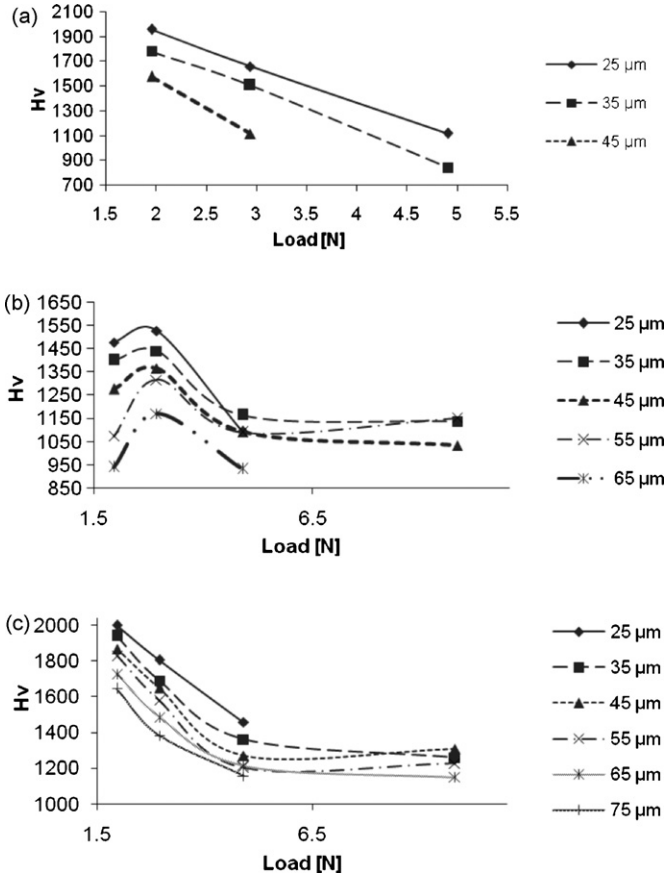

Fig. 4. Microhardness as a function of the indentation loads from the different distances from the surface of the borided layer at the temperatures of: (a) 1173 K, (b) 1223 K and (c) 1273 K.

compressive stresses induced by boriding increase as a function of the distance from the surface until a critical distance is reached (80 μm approximately) then the compressive stresses decrease, and in the substrate they change to tensile stresses.[1] On the other hand, according to Galibois et al. [21], the thermal residual compression stresses caused by the growth of the iron boride layer and the differences of the specific volume between the matrix and the Fe_2B[2] phase are factors to be considered in the microhardness values at the different distances from the surface. The residual stresses (σ_{th}) occurring in thin layers can be calculated by the formula (see [22] and references therein):

$$\sigma_{th} = \frac{E}{1-v}(\alpha_l - \alpha_s)(T_b - T_0) \quad (1)$$

where E is the Young's modulus of the Fe_2B boride layer which is assumed constant with a continuous texture degree equal to 1 [23], α_l the thermal expansion coefficient of the layer equal to $6.5 \times 10^{-6}\,^{\circ}C^{-1}$, α_s equal to $11.96 \times 10^{-6}\,^{\circ}C^{-1}$, T_b the treatment temperature and T_0 is the room temperature. Eq. (1) is a simplified relationship which permits us to estimate the thermal residual stresses in elastic isotropic thin layers.

The aforementioned equation gives the distributions of the stresses parallel to the surface, and do not consider the perpendicular ones. The data obtained according to Eq. (1), reveal that the stresses occurring in the monophase borided layers (Fe_2B)

[1] The presence in the coatings of [0 0 1] axial crystallographic texture leads to a decrease in the absolute value of the compressive stresses occurring in the layers, which with an increase in the degree of texture of the boride phases gradually transform to tensile stresses.

[2] The specific volume of the Fe_2B is 0.1363 cm^3/g compared with the value of 0.1276 cm^3/g for the AISI 1045 steel matrix.

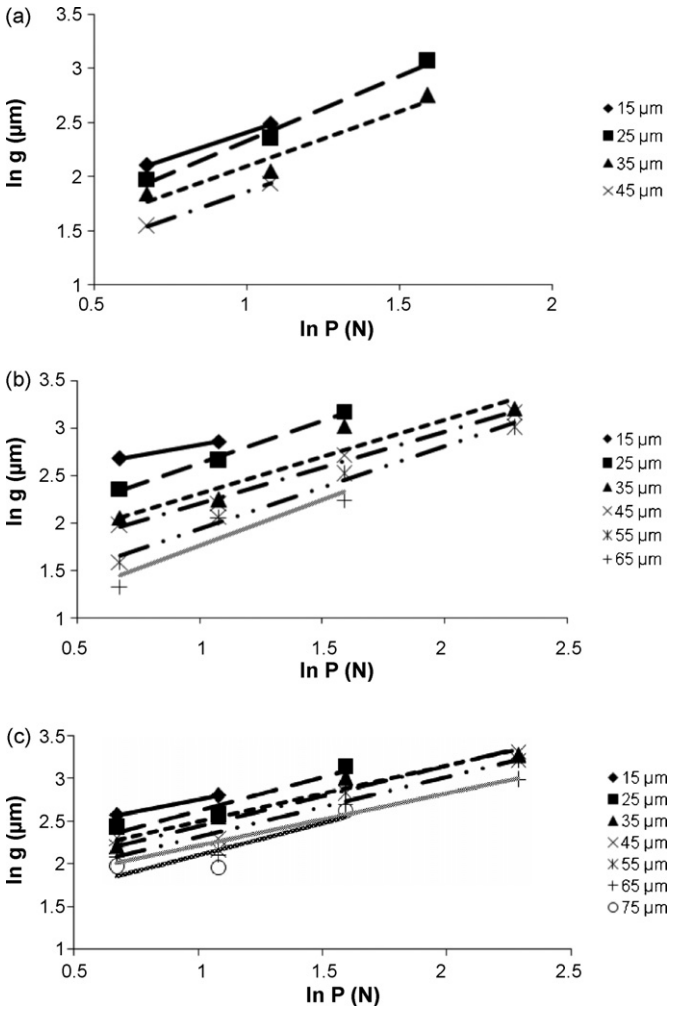

Fig. 5. Relationship between the crack length and the indentation loads for the boriding temperatures of: (a) 1173 K, (b) 1223 K and (c) 1273 K.

are compressive with magnitudes ranging from −1640 MPa for the temperature of 1123 K to −1939 MPa for the temperature of 1273 K.

The presence of Palmqvist cracks generated by the Vickers microindentation tests at the Fe_2B boride layers are established by the slopes obtained from the graphs ln g against ln P as shown in Fig. 5. The slope values are approximately in the range of 1/2 and 1, where the formation of the Palmqvist cracks may be mechanically equivalent to a semi-infinite crack loaded by a force P at a distance g from the crack tip [6,24]. On the other hand, Table 2 shows the characteristic lengths, g and c $(l+g)$, for the different applied loads and microindentation distances at the temperature of 1273 K

The fracture toughness evaluation of the Fe_2B boride layer was determined by means of the models used by Laugier [13] and Niihara et al. [14]. Both models use the indentation test load, the crack length, the indentation size, the elastic modulus, and the hardness of the material. These parameters are raised to non-integer exponents such as 0.4, 0.6 and 0.7. In other applicable equations, the same parameters are raised to 0.5, 1.5 or 2.0. The difference between the models PI and PII are the coefficient values represented by each equation, which are empirically determined by the calibration of the K_c value with conventional and standardized methods. The Vickers indentation fracture models proposed in this work are based on the assumption that there are no pre-existing surface stresses. Nevertheless, it is necessary to taking account the presence of residual stresses at the boride layer which is a factor to be considered when applying the Vickers indentation test. In this case, the apparent surface crack length is a reflection of both the fracture toughness of the phase and any pre-existing residual stresses, be they compressive or tensile, without considering the applied load. A compressive residual stress will decrease the surface crack length relative to the equilibrium length in the absence of residual stresses; a tensile stress will do the reverse (see [25] and references therein). Then, the fracture toughness values of the Fe_2B phase obtained by both models are sensible to the accuracy to which the crack lengths can be measured (and hence to which the fracture toughness can be calculated), being necessary to discard unacceptable crack patterns occurring from the sides of the indentation instead of the corners (parallel to the surface) and crack branching.

As stated by Byakova [26], the anisotropy of the boride layers is influenced by the crystallographic composition (columnar crystals) and also by the presence of the residual stresses, so, the fracture toughness should be measured considering cracks normal and parallel to the surface. What is more, the brittle fracture criteria are not sensitive to the residual stresses when the cracks do not intersect a grain boundary. As a consequence, the fracture resistance is directly related to the structural non-uniformity of the boride coating. For this reason the critical stress

Table 2
Characteristic lengths of g and c for different microindentation loads and distances from the surface for the Fe_2B borided layer formed at 1273 K

Distance from the surface (μm)	1.96		2.94		4.91		9.81	
	g (μm)	c (μm)	g (μm)	c (μm)	g (μm)	c (μm)	g (μm)	c (μm)
P (N)								
15	12.9 ± 2.0	19.5 ± 2.2	16.1 ± 3.9	24.6 ± 3.8	–	–	–	–
25	11.1 ± 1.4	17.9 ± 1.4	12.8 ± 3.0	21.6 ± 3.0	22.7 ± 4.4	35.3 ± 4.7	–	–
35	9.0 ± 1.5	15.9 ± 1.6	12.6 ± 2.9	21.7 ± 3.0	19.9 ± 3.0	33.0 ± 3.1	25.9 ± 4.2	45.2 ± 4.1
45	9.8 ± 3.2	16.9 ± 3.2	9.8 ± 2.4	19.0 ± 2.3	19.8 ± 6.7	33.3 ± 6.5	27.0 ± 6.5	45.8 ± 6.4
55	8.9 ± 2.5	16.0 ± 2.6	8.6 ± 2.5	18.0 ± 2.4	16.5 ± 3.3	30.4 ± 3.3	24.5 ± 6.0	44.0 ± 6.0
65	7.9 ± 1.9	15.3 ± 1.9	8.1 ± 1.8	17.8 ± 1.8	14.5 ± 3.3	28.3 ± 3.2	19.3 ± 4.1	39.5 ± 3.9
75	7.0 ± 1.1	14.5 ± 1.2	7.0 ± 1.8	17.2 ± 1.8	13.6 ± 5.2	27.8 ± 5.1	–	–

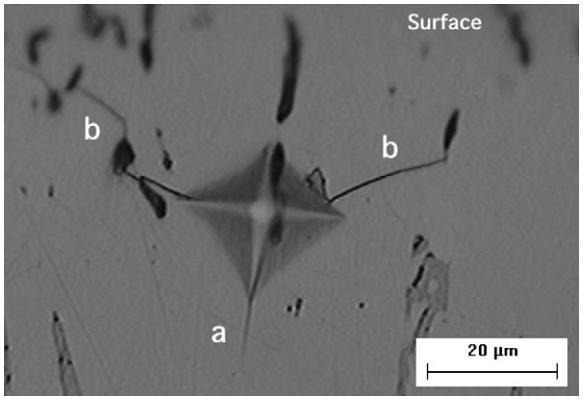

Fig. 6. Palmqvist cracks produced by Vickers microindentation: (a) normal to the surface and (b) parallel to the surface.

intensity factor should be presented as K_c (θ) where θ is the coordinate angle between the direction of crack propagation and the surface.

The fracture toughness evaluated with normal cracks K_c (90°) to the surface is 30–80% higher than that evaluated with parallel cracks K_c (0°), and when $P_{002} \geq 2.5$,[3] K_c (90°) reaches the level of K_c (0°); expecting similar lengths for both cracks (parallel and normal to the surface). Due to the fact that the cracks normal to the surface are shorter than the parallel ones or even do not appear (Fig. 6), it is assumed that the critical condition mentioned before ($P_{002} \geq 2.5$) has not been reached and therefore the K_c value in the parallel direction will be the critical value of the fracture toughness of the Fe_2B boride layer. In fact, equal length of cracks for all four of indentor impression tips is only observed in tests on surface layers which are isotropic in structure and stresses. Thus, the K_c values of the equations proposed in Table 1 are determined using only cracks parallel to the surface. Due to the fact that the fracture toughness is higher in the direction normal to the surface, it is assumed that the compressive stresses are higher in the normal direction and retards the crack growth produced by microindentation. Another important feature of this

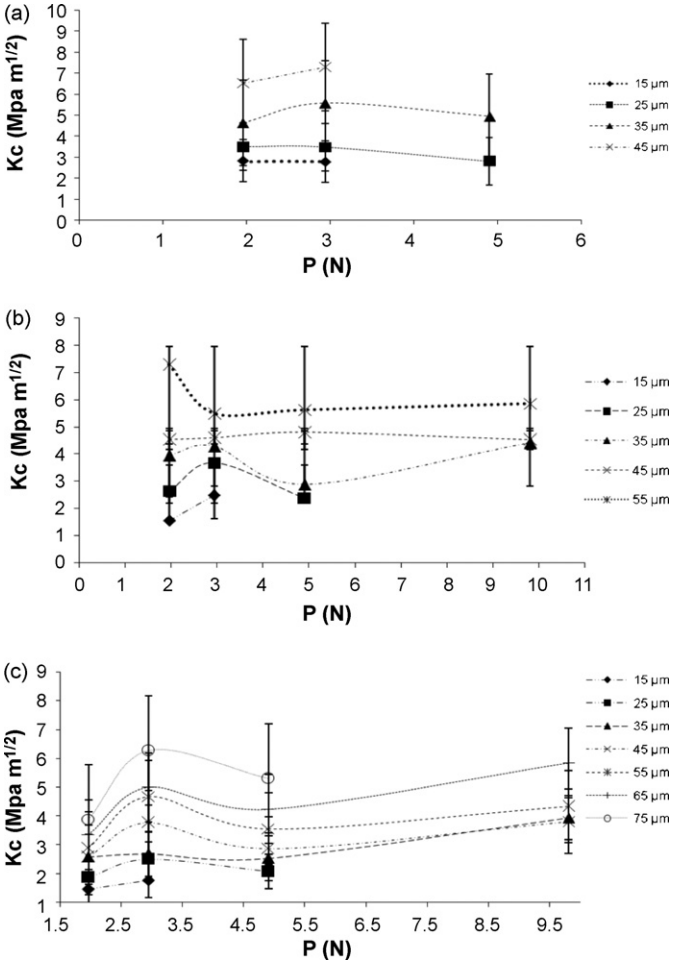

Fig. 7. Behavior of K_c (PI model) against the indentation load for the boriding temperatures of: (a) 1173 K, (b) 1223 K and (c) 1273 K.

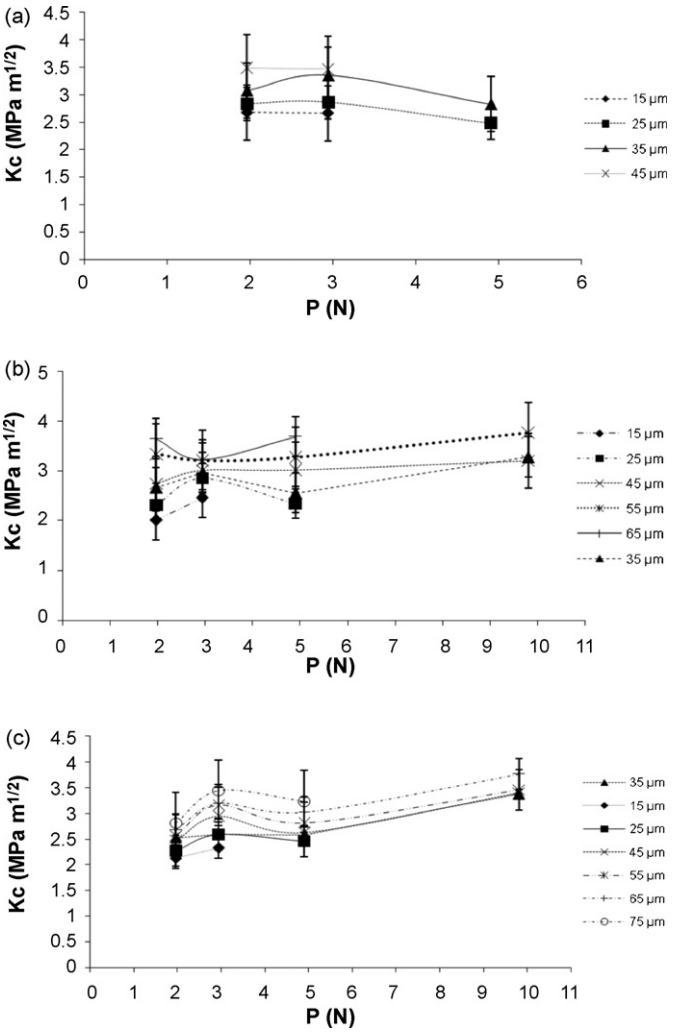

Fig. 8. Behavior of K_c (PII model) against the indentation load for the boriding temperatures of: (a) 1173 K, (b) 1223 K and (c) 1273 K.

[3] The pole density P_{hkl} is the ratio of the number of crystals for which the [$h\,k\,l$] axis of texture which is a normal to the [$u\,v\,w$] plane coincides with the normal to the surface of the specimen to the number of crystals of the same orientation in a texture-free specimen [25].

crack propagation pattern is that there is no evidence of crack deflection or another toughening mechanism.

A fundamental problem with the Vickers indentation fracture toughness tests, as stated by Quinn and Bradt [27] is that brittle materials[4] do not deform and fracture underneath an indentation in a self-similar manner to the crack models proposed in this study. In the PI model case, the cracks are considered in a semi-elliptical form in comparison to the semicircles cracks proposed in PII.

Figs. 7 and 8 show the behavior of the K_c values against the Vickers indentation testing loads. As the distance from the surface increases, so the K_c values, as previously discussed. However, both models do not propose a unique value to determine the fracture toughness of the Fe_2B boride phase. Likewise, the K_c results for the PII model (mean value of $4.1 \pm 0.6\,\mathrm{MPa\,m^{1/2}}$) are more stable in comparison with the PI model ($4.5 \pm 1.8\,\mathrm{MPa\,m^{1/2}}$) according to the applied loads used in this work. Furthermore, the different microindentation distances from the surface of the borided samples, the treatment temperatures, the boride layer thicknesses and the crack length measurements as a function of thermal residual stresses produced by the boride growth seem to influence the fracture toughness value of the Fe_2B phase. Obviously the values of K_c recorded under these conditions characterize the fracture toughness of the individual grains but do not reflect the fracture resistance of the whole coating as an elastic continuum as a whole.

4. Conclusions

This study evaluated the fracture toughness of the Fe_2B boride layer using the Palmqvist crack models proposed by Laugier and Niihara et al. [13,14]. The presence of Palmqvist cracks at the boride layers is established by the slope values obtained between 1/2 and 1 in the applied load versus crack length curves. The fracture toughness values obtained by the PII model indicate minor dispersion in comparison with the PI model. Hence, the difference between the models PI and PII are the coefficient values represented by each equation, which are empirically determined by the calibration of the K_c value with conventional and standardized methods.

The results obtained for both models do not indicate a constant value for the fracture toughness of the iron boride, as that parameter is influenced by the microindentation distances, the boriding temperatures, the thickness of the boride layer and the apparent surface crack length that is a reflection of both the fracture toughness of the phase and any pre-existing residual stresses. In this case, for the evaluation of the brittle strength of boride non-uniformity coatings, it is desirable to use the critical stress intensity factors presented in the form of the function $K_c\,(\theta)$, where $0^\circ \leq \theta \leq 90^\circ$ is the coordinate angle between the direction of crack propagation and the surface. Therefore it is important to formulate brittle fracture criteria in boride layers for determining K_c invariant with elastic residual stresses operating within them for the different experimental conditions of the boriding process.

[4] In Ref. [17], Campos et al. have determined by means of the AFM technique, that the Fe_2B iron boride is constituted by fine crystals, which possibly causes the layer not to deform and fracture in the same manner based on the criteria established by the Palmqvist crack models.

Acknowledgments

This work has been supported by the research grant 53859 of *Consejo Nacional de Ciencia y Tecnología* at Mexico. I. Campos thanks the project 20070130 chair supported by the *Secretaría de Investigación y Posgrado* of the Instituto Politécnico Nacional.

References

[1] I. Campos, O. Bautista, G. Ramírez, M. Islas, J. de la Parra, L. Zuñiga, Appl. Surf. Sci. 243 (2005) 429–436.
[2] I. Campos, R. Torres, O. Bautista, G. Ramírez, L. Zuñiga, Appl. Surf. Sci. 252 (2006) 2396–2403.
[3] E. Meléndez, I. Campos, E. Rocha, M.A. Barrón, Mater. Sci. Eng. A 234-236 (1997) 900–903.
[4] A.K. Sinha, Boronizing, ASM Handbook, OH, USA, J. Heat Treat. 4 (1991) 437.
[5] A. Graf von Matuschka, Boronising, Carl Hanser Verlag, Munich, FRG (1980).
[6] C.B. Ponton, R.D. Rawlings, Mater. Sci. Technol. 5 (1989) 865–872.
[7] C.B. Ponton, R.D. Rawlings, Mater. Sci. Technol. 5 (1989) 961–976.
[8] I. Uslu, H. Comert, M. Ipek, O. Ozdemir, C. Bindal, Mater. Design 28 (2007) 55–61.
[9] I. Ozbek, C. Bindal, Surf. Coat. Technol. 154 (2002) 14–20.
[10] U. Sen, S. Sen, F. Yilmaz, Mater. Proc. Technol. 148 (2004) 1–7.
[11] S. Sen, I. Ozbek, U. Sen, C. Bindal, Surf. Coat. Technol. 135 (2001) 173–177.
[12] N. Frantzevich, F.F. Voronov, S.A. Bakuta, Elastic Constants and Elastic Modulus for Metals and Non-metals: Handbook, 1st ed., Naukova Dumka Press, Kiev, 1982.
[13] M.T. Laugier, J. Mater. Sci. Lett. 6 (1987) 355–356.
[14] K. Niihara, R. Morena, D.P.H. Hasselman, J. Mater. Sci. Lett. 1 (1982) 13–16.
[15] R. Torres, I. Campos, G. Ramírez, O. Bautista, J. Martínez, IJMMP 2 (2007) 73–83.
[16] H. Kunst, O. Schaaber, Harterei-Technik Mitt. 26 (1971) 18–20.
[17] I. Campos, M. Islas, G. Ramírez, C. VillaVelázquez, C. Mota, Appl. Surf. Sci. 253 (2007) 6226–6231.
[18] F. Sergejev, M. Antonov, Proc. Estonian Acad. Sci. Eng. 12 (2006) 388–398.
[19] Z. Li, A. Ghosh, A. Kobayashi, R.C. Bradt, J. Am. Ceram. Soc. 72 (1989) 904–911.
[20] B.V. Babushkin, P.Z. Polyakov, Metallovedenie i Termicheskaya Obrabotka Metallov 7 (1973) 27–30.
[21] A. Galibois, O. Boutenko, B. Voyzelle, Acta Metall. 28 (1980) 1753–1763.
[22] D. Golanski, A. Marczuk, T. Wierzchon, J. Mater. Sci. Lett. 14 (1995) 1499–1501.
[23] L.S. Lyakhovich, L.N. Kosachevskii, A.Ya. Kulik, V.V. Surkov, Yu.V. Turov, Fiziko-Khimicheskaya Mekhankika Materialov 9 (1973) 34–37.
[24] B.E. Meacham, M.C. Marshall, D.J. Branagan, Metall. Mater. Trans. A 37 (2006) 3617–3626.
[25] B. Lawn, E.R. Fuller, J. Mater. Sci. 19 (1984) 4061–4067.
[26] A.V. Byakova, Poroshkovaya Metallurgiya 4 (1993) 36–43.
[27] G.D. Quinn, R.C. Bradt, J. Am. Ceram. Soc. 90 (2007) 673–680.